Two-step pathway for isoprenoid synthesis

Alkiviadis Orfefs Chatzivasileiou (Αλκιβιάδης Ορφεύς Χατζηβασιλείου)[a], Valerie Ward[a,b], Steven McBride Edgar[a], and Gregory Stephanopoulos[a,1]

[a]Department of Chemical Engineering, Massachusetts Institute of Technology, Cambridge, MA 02139; and [b]Department of Chemical Engineering, University of Waterloo, Waterloo, ON N2L 3G1, Canada

Edited by Alexis T. Bell, University of California, Berkeley, CA, and approved November 21, 2018 (received for review July 31, 2018)

Isoprenoids comprise a large class of chemicals of significant interest due to their diverse properties. Biological production of isoprenoids is considered to be the most efficient way for their large-scale production. Isoprenoid biosynthesis has thus far been dependent on pathways inextricably linked to glucose metabolism. These pathways suffer from inherent limitations due to their length, complex regulation, and extensive cofactor requirements. Here, we present a synthetic isoprenoid pathway that aims to overcome these limitations. This isopentenol utilization pathway (IUP) can produce isopentenyl diphosphate or dimethylallyl diphosphate, the main precursors to isoprenoid synthesis, through sequential phosphorylation of isopentenol isomers isoprenol or prenol. After identifying suitable enzymes and constructing the pathway, we attempted to probe the limits of the IUP for producing various isoprenoid downstream products. The IUP flux exceeded the capacity of almost all downstream pathways tested and was competitive with the highest isoprenoid fluxes reported.

isoprenoids | biosynthesis | isopentenol | utilization | pathway

Isoprenoids are a large class of over 50,000 natural compounds found in plants and many living organisms (1). They are of significant interest due to their varied applications in fields spanning medicine, agriculture, flavors, fragrances, cosmetics, and nutrition (1). All naturally produced isoprenoids are derived from two C_5 isoprenoid precursors, isopentenyl diphosphate (IPP) and its isomer dimethylallyl diphosphate (DMAPP). These precursors are condensed through sequential addition to generate larger isoprenoid precursor molecules, like geranyl diphosphate (GPP, C_{10}), farnesyl diphosphate (FPP, C_{15}), and geranylgeranyl diphosphate (GGPP, C_{20}). These prenyl diphosphate backbones can be further functionalized by terpene synthases and cytochrome P_{450} monooxygenases. Isoprenoid precursors DMAPP and IPP are naturally produced in the cell through one of two pathways (2). The mevalonate (MVA) pathway involves seven reactions to produce IPP from acetyl-CoA. DMAPP is then produced through the isomerization of IPP by the enzyme isopentenyl-pyrophosphate delta isomerase (IDI). The second pathway is the nonmevalonate pathway (MEP or DXP pathway), which starts from the condensation of equimolar quantities of pyruvate and glyceraldehyde 3-phosphate (G3P) and produces both DMAPP and IPP at a ratio of ∼5:1 after seven reactions (2, 3).

These natural pathways have many limitations that must be overcome for them to perform optimally. Concerning the MEP pathway, imbalances in the supply of G3P and pyruvate can create bottlenecks, leading to decreased pathway performance (4). Furthermore, the iron-sulfur enzymes IspG and IspH are sensitive to oxygen (5), and their inactivation leads to carbon loss, due to accumulation and excretion of metabolic intermediates, such as 2-C-methyl-D-erythritol 2,4-cyclodiphosphate (MEC) (6). Pathway intermediates or downstream products have been shown to inhibit "gate keeper" enzymes in both the MEP and the MVA pathways, with IPP inhibiting 1-deoxy-D-xylulose 5-phosphate (DXP) synthase (7); CoA, acetylacetyl-CoA, and HMG-CoA inhibiting HMG-CoA synthase (8); HMG, free CoA, and NAD(P)$^+$/NADPH inhibiting HMG-CoA reductase (9, 10); and IPP, DMAPP, GPP, and FPP inhibiting mevalonate kinase (11). This complex regulation can hinder attempts to up-regulate either pathway. Finally, at a systems level, both the MVA and the MEP pathways require multiple cofactors, like ATP, CTP, NADH, and NADPH, as well as precursors for IPP synthesis from central carbon metabolism, thereby competing with other cellular processes for resources, which can complicate attempts to increase isoprenoid pathway flux. Several attempts at engineering bypass pathways to alleviate some of the challenges associated with highly regulated enzymes have been made (12, 13); however, these attempts still rely on entry points within the MEP or MVA pathways. Here, we report a synthetic pathway for the biosynthesis of isoprenoids from a secondary substrate, termed the isopentenol utilization pathway (IUP), which produces isoprenoid precursors IPP and DMAPP from isopentenol isomers isoprenol or prenol (Fig. 1*A*). We found that the IUP is a metabolic pathway whose flux is competitive with some of the fastest reported isoprenoid pathways and allows us to decouple isoprenoid biosynthesis from central carbon metabolism, something which will tremendously simplify future engineering endeavors for production of high value isoprenoids.

Results

Isopentenol isomers were chosen as precursors to IPP and DMAPP due to their structural similarities. In the first step, isoprenol or prenol is phosphorylated to form isopentenyl monophosphate (IP) or dimethylallyl monophosphate (DMAP), respectively, and, in the second step, IP or DMAP is phosphorylated again to form IPP or DMAPP, respectively. The second step of the pathway is known to be catalyzed by isopentenyl phosphate kinase (IPK), which is a part of the archaeal mevalonate pathway (14). Although the first phosphorylation does not occur in nature, some phosphokinases can exhibit promiscuous kinase activity (15, 16). We therefore screened several kinases for isopentenol kinase activity, including IPK homologs, as a recent report suggested that some IPK variants can

Significance

Isoprenoids are a class of natural products with applications in many fields, including medicine and agriculture. Biosynthesis of isoprenoids has emerged as the most commercially viable option for their mass production. We report the creation of an enzymatic pathway for the biological production of isoprenoids, which uses externally provided isoprenol as its substrate instead of a glucose-derived catabolite, making it radically different from naturally occurring pathways or their engineered variants. The pathway is only two steps long and uses a single cofactor, ATP. Our results show that it is decoupled from central carbon metabolism and can sustain a very high flux. These advantages make it a noteworthy alternative to known isoprenoid pathways.

Author contributions: A.O.C., V.W., S.M.E., and G.S. designed research; A.O.C. and V.W. performed research; V.W. contributed new reagents/analytic tools; A.O.C. and V.W. analyzed data; and A.O.C. wrote the paper.

Conflict of interest statement: The authors are listed as inventors in a pending patent application (no. US 62/677,421; applicant, Massachusetts Institute of Technology) encompassing all the information presented here, as well as additional applications.

This article is a PNAS Direct Submission.

[1]To whom correspondence should be addressed. Email: gregstep@mit.edu.

This article contains supporting information online at www.pnas.org/lookup/suppl/doi:10.1073/pnas.1812935116/-/DCSupplemental.

Published online December 24, 2018.

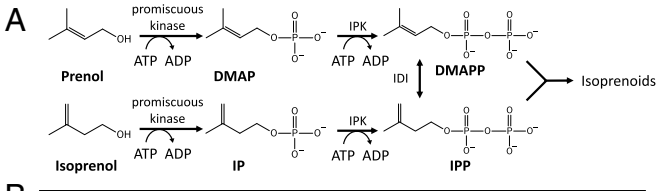

B

Enzyme candidate	Source	Abbrev.
Isopentenyl Phosphate Kinase	*H. volcanii*	HvIPK
Isopentenyl Phosphate Kinase	*M. thermoautotrophicus*	MtIPK
Isopentenyl Phosphate Kinase	*M. janaschii*	MjIPK
Isopentenyl Phosphate Kinase	*T. acidophilium*	TaIPK
Isopentenyl Phosphate Kinase	*T. acidophilium* – V73I + Y141V + K204G	TaIPK-3m
Mevalonate Kinase	*S. cerevisiae*	ScMK
Glycerol Kinase	*E. coli*	EcGK
Homoserine Kinase	*E. coli*	EcHK
Choline Kinase	*S. cerevisiae*	ScCK

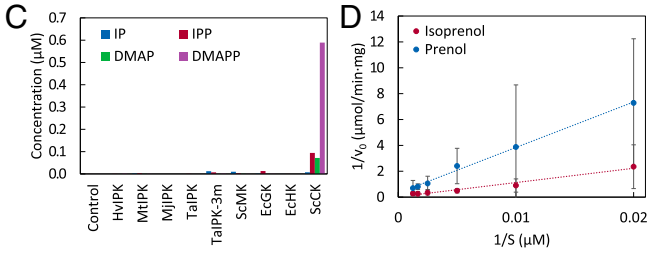

Fig. 1. Development of the isopentenol utilization pathway and in vitro characterization of choline kinase. (*A*) The IUP can produce the basic isoprenoid metabolic intermediates IPP and DMAPP in two steps using isoprenol or prenol, respectively, as feedstock. The steps are catalyzed by a promiscuous kinase and isopentenyl phosphate kinase (IPK). IPP and DMAPP can then be interconverted via IDI. IPP and DMAPP act as the precursor molecules for larger prenyl diphosphates and eventually isoprenoids. (*B*) Enzymes screened in this work. (*C*) Results of overnight screen to identify a suitable promiscuous kinase using isoprenol (IP and IPP) or prenol (DMAP and DMAPP) as a substrate, respectively. (*D*) Kinetic analysis of choline kinase from *S. cerevisiae* (ScCK) at a fixed ATP concentration for the determination of k_{cat} and K_m with regard to isopentenol substrate. Reaction rates are reported as means ± SD ($n = 3$).

convert prenol to DMAP through promiscuous activity (17), along with other kinases selected based on the similarity of their natural substrates to isoprenol or prenol (Fig. 1*B*). After purification, these enzymes were screened for isopentenol kinase activity in vitro (18).

While several enzymes were capable of converting isoprenol to IP after an overnight incubation period (Fig. 1*C*), only choline kinase from *Saccharomyces cerevisiae* (ScCK) was capable of producing appreciable amounts of both IP and DMAP. Interestingly, ScCK was also able to catalyze the second phosphorylation step, forming IPP and DMAPP. However, very little IPP or DMAPP was detected after a shorter incubation (~90 min), suggesting a preference for the first step of the pathway (*SI Appendix*, Fig. S1). Kinetic studies using the purified enzyme revealed that ScCK operates at an optimal pH of 7.5 and an optimal temperature of 34 °C to 38 °C (*SI Appendix*, Fig. S1). The enzyme displayed a Michaelis–Menten constant (K_M) of 4,539 or 1,113 μM and k_{cat} of 14.7 or 1.1 s^{-1} at 37 °C when the substrate was isoprenol or prenol, respectively (Fig. 1*D*). ScCK was paired with an IPK from *Arabidopsis thaliana* (AtIPK) to catalyze the second step of the pathway as it had the highest reported k_{cat}/K_M (14). To balance the ratio of IPP and DMAPP, an IDI was included. The complete isopentenol utilization pathway (IUP) is thus composed of the enzymes ScCK, AtIPK, and IDI and requires ATP as its sole cofactor.

Isoprenoids are necessary for cell survival and perform essential cellular functions, including electron transport and maintenance of membrane fluidity (19). To create an in vivo proof of concept, we tested the ability of the IUP to rescue a nonviable MEP-knockout strain incapable of producing isoprenoids via its native MEP pathway. Using the CRISPR-Cas9 system (20, 21), we created an MEP-knockout strain, KO1, in which the *ispG* gene is removed, rendering it unable to synthesize the MEP pathway intermediate (E)-4-Hydroxy-3-methyl-but-2-enyl pyrophosphate (HMBPP), while growth can be rescued via the lower mevalonate pathway encoded by the genes *erg12*, *erg8*, and *mvd1* on the plasmid pBAD33-proA-MEVI when mevalonate is supplied in minimal media (*SI Appendix*, Fig. S2). We created two plasmids for the expression of the IUP to test its ability to act as a sole provider of isoprenoids. The first used the Standard European Vector Architecture (22) to clone the IUP operon under the control of the constitutive promoter P_{pro4} (23), creating the plasmid pSEVA228-pro4IUPi (herein called "pro4IUP"). The second, pTET-IUPi, herein called "pTETIUP," places control of the IUP under the strong inducible anhydrotetracycline (aTC) promoter P_{TET} (24). The difference in strength of these expression systems was confirmed by green fluorescent protein expression (*SI Appendix*, Fig. S3). KO1 was transformed with either pro4IUP or pTETIUP plasmids to create strains KO2 or KO3, respectively. Strain KO1 was not viable in minimal media or minimal media supplemented with isoprenol or prenol but was viable in minimal media supplemented with 1 mM mevalonate. When supplemented with 0.6 mM isoprenol in the absence of mevalonate or HMBPP, both KO2 and KO3 grew after lag periods of 36 h, compared with WT *Escherichia coli*, which exhibited a lag period of 2 h, and exponential growth rate shown in *SI Appendix*, Fig. S4. IUP is thus sufficiently expressed in *E. coli* to be used as the sole isoprenoid pathway and an alternative to the MEP or the MVA pathways. All subsequent experiments expressed the IUP in WT *E. coli*.

We further characterized pathway strength by combining the IUP with a downstream module for lycopene synthesis. Lycopene is the C_{40} isoprenoid responsible for the coloration of tomatoes (25) and can be readily quantified using UV/Vis spectroscopy. For quantification purposes, a fresh lycopene standard was generated in the laboratory using a standard procedure (26) as lycopene is known to degrade rapidly due to oxidation, heat, and/or light during storage (27), leading to bleaching of the standard and overestimation of lycopene titers. We partitioned the upstream (IUP) and downstream (lycopene synthesis) genes into two operons carried on separate plasmids. The lycopene plasmid pAC-LYCipi encoded genes required for the production of lycopene (*crtE*, *crtB* and *crtI*) and a copy of *idi* from *Enterobacter agglomerans* (28). The lycopene plasmid was transformed alone (control) or in combination with the pro4IUP or pTETIUP plasmids. After culturing in

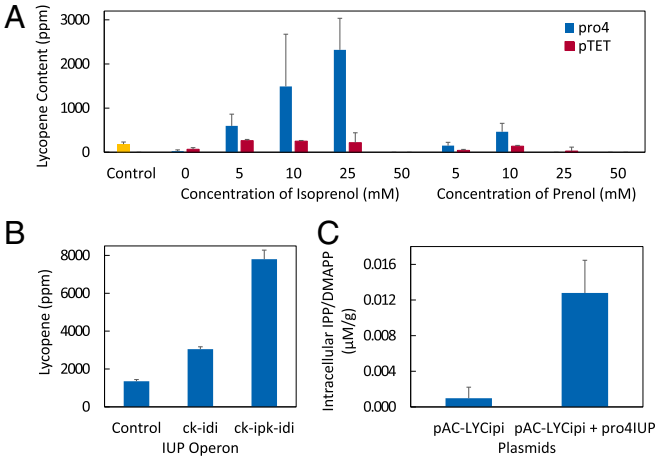

Fig. 2. Characterization of the IUP using the lycopene pathway encoded by pAC-LYCipi in M9 media. (*A*) Lycopene content in strains containing the IUP under the control of a low strength constitutive promoter (pro4) or a strong inducible promoter (pTET) induced with 20 ng/mL aTc. This was compared with the control strain containing only the lycopene production plasmid (pAC-LYCipi), without the IUP plasmid or addition of either isopentenol. (*B*) The effect of *ipk* gene on the synthesis of lycopene. (*C*) The effect of the pro4IUP pathway on intracellular levels of IPP/DMAPP compared with the control strain containing only pAC-LYCipi. All experimental values are normalized to dry cell weight and represent the mean ± SD of three biological replicates.

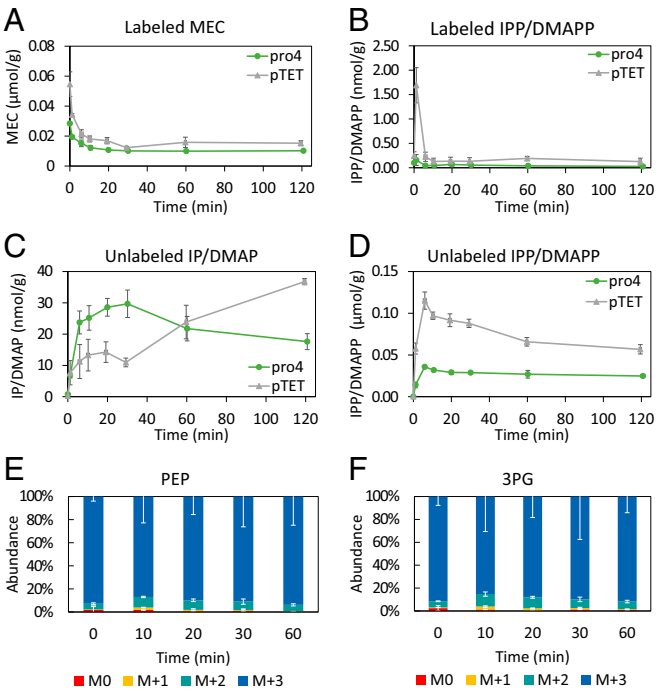

Fig. 3. Isoprenol pulse–chase experiment for metabolite monitoring. (*A*) Levels of labeled MEC. (*B*) Levels of labeled IPP/DMAPP. (*C*) Levels of unlabeled IP/DMAP. (*D*) Levels of unlabeled IPP/DMAPP. (*E* and *F*) Labeling patterns for 3-phosphoglycerate (3PG) and phosphoenolpyruvate (PEP), respectively, in the pro4IUPi strain over the first 60 min. pTET cultures were induced with 10 ng/mL aTC. All experimental values are normalized to dry cell weight and represent the mean ± SD of three biological replicates.

different concentrations of prenol or isoprenol in M9 media for 48 h, lycopene content was quantified. The highest lycopene titer was observed using 25 mM isoprenol (Fig. 2*A*).

Removing the *ipk* gene from the IUP operon was found to significantly decrease lycopene titers (Fig. 2*B*), signifying that an IPK is essential for a well-functioning IUP. There was still a significant pool of IPP/DMAPP in the pro4IUP strain, despite the expression of the lycopene genes, suggesting a mismatch in flux generated by IUP and converted into lycopene (Fig. 2*C*). To estimate the flux generated by pro4 and pTET IUP strains lacking a downstream cassette, we grew them at 37 °C in M9 media using uniformly ^{13}C-labeled glucose as the sole carbon source. During stationary phase, unlabeled isoprenol was pulsed in, and pTETIUP cultures were induced to start production of the IUP enzymes (Fig. 3).

Immediately before the addition of unlabeled isoprenol, we detected fully labeled MEC, an MEP-pathway metabolite that is known to accumulate in *E. coli* (6) (Fig. 3*A*), as well as a small amount of fully labeled isopentenyl pyrophosphate (Fig. 3*B*). No unlabeled isopentenyl monophosphate (IP) or pyrophosphate (IPP) was detected (Fig. 3 *C* and *D*). Within minutes of isoprenol addition, concentrations of unlabeled IP and IPP rapidly increased to levels significantly higher than those of the native MEP pathway (labeled IPP/DMAPP at t = 0) (Fig. 3 *C* and *D*). The concentration of labeled IPP quickly dropped to barely detectible levels while the concentration of labeled MEC also decreased (Fig. 3 *A* and *B*), indicating possible feedback inhibition of the MEP pathway by high concentrations of IPP, as previously reported (7). By fitting a simple first-order mathematical model (described in *SI Appendix*) to the total measured concentrations of IPP, we estimated IPP flux generated by the IUP. The largest IPP flux [4.93 μmol/(g_{dcw}•h); sum of squared residuals (SSR) = 4.7·10^{-4} μmol^2/g_{dcw}^2] occurred under the control of the P_{TET} promoter (induced with 10 ng/mL aTC). We also observed that the labeling patterns of the glycolytic intermediates phosphoenolpyruvate (PEP) and 3-phosphoglyceric acid (3PG) remained unchanged after the isoprenol pulse (Fig. 3 *E* and *F*), suggesting that the IUP is uncoupled from main glycolysis.

We thus established that expression of the IUP can lead to IPP accumulation higher than that produced by the MEP pathway. Furthermore, even in cells harboring the (high flux) lycopene pathway, significant accumulation of precursors IPP/DMAPP was observed. These observations suggest a high flux through the IUP; hence, we wanted to next probe the limits of the IUP flux through the synthesis of other isoprenoid compounds. To this end, we transformed both the IUP plasmids along with plasmids containing downstream operons for the production of valencene, limonene, miltiradiene, amorphadiene, and taxadiene (*SI Appendix*, Table S1). In all cases except valencene, addition of the IUP led to statistically significant higher isoprenoid titers ($P < 0.01$) (Fig. 4*A*).

Previous results indicated that the lycopene operon from pAC-LYCipi was not sufficient to completely utilize the flux from the pro4IUP plasmid (Fig. 2*C*). Therefore, we created variants with different copy numbers (p5T7-LYCipi ~ 5, pAC-LYCipi ~ 15, p20-LYCipi ~ 20, pUC-LYCipi > 100) and promoter strengths (endogenous constitutive promoter vs. T7 inducible promoter) and transformed them alone or in combination with either pro4IUP or pTETIUP. Cells were cultured in M9 media supplemented with 0.5% (wt/vol) casamino acids in serum bottles, and lycopene production was monitored until a maximum lycopene content was reached (Fig. 4*B*). When the endogenous constitutive promoter was used, cells took 48 h to reach their maximum lycopene content. However, increasing the plasmid copy number to ~20 using the pBR322 origin of replication increased lycopene content more than threefold. When the T7 promoter was used, lycopene productivity was increased by over 17-fold in the pro4 strain from the original pAC-LYCipi pro4IUP stain, reaching maximum lycopene content within 8 h. We also noted a small decrease in cell concentration in cultures expressing the IUP, attributable to the presence of isoprenol in the media (*SI Appendix*, Fig. S5). To establish whether the IUP or the downstream operons

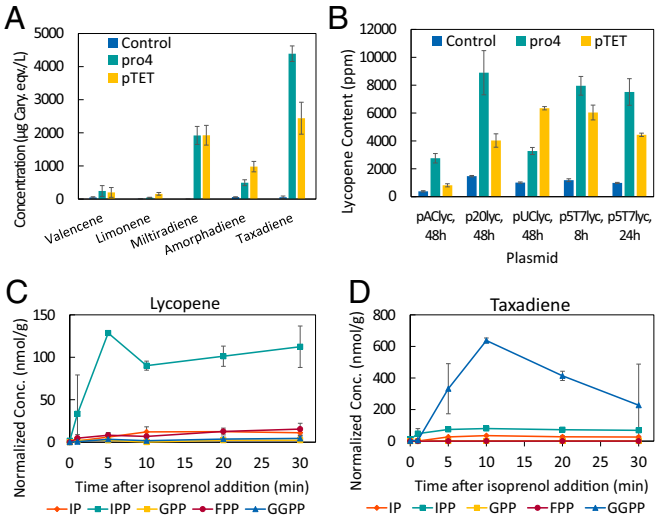

Fig. 4. Use of the isopentenol utilization pathway for the production of isoprenoids. (*A*) Isoprenoid product titers after culturing for 48 h expressing the IUP under the control of the pro4 or pTET promoters (10 ng/mL aTC), along with a control expressing only the downstream cassette. Concentrations are expressed as equivalents of the internal standard caryophyllene. (*B*) Lycopene content in strains using an endogenous constitutive promoter with various copy number plasmids (pAC-LYCipi ~ 15, p20-LYCipi ~ 20, pUC-LYCipi > 100) and under the control of a strong inducible promoter in a plasmid with copy number ~5 (p5T7-LYCipi). (*C* and *D*) Concentrations of metabolic intermediates for strains expressing the IU pathway along with a plasmid for the production of (*C*) lycopene (p5T7-LYCipi) or (*D*) taxadiene (p5T7tds-ggpps), respectively. All metabolite and product concentrations are reported as means ± SD of three biological replicates. Conc., concentration.

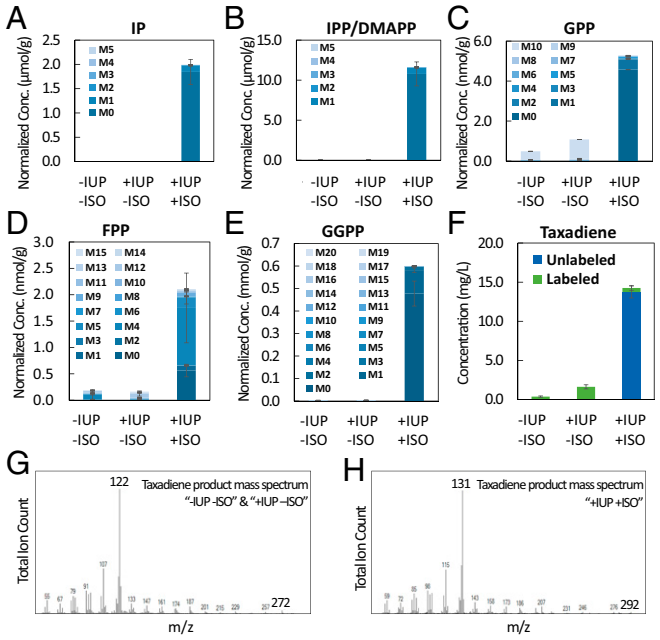

Fig. 5. Metabolite levels and products from cultures with taxadiene-producing strains growing in U-^{13}C–labeled glucose. The cultures differ on whether they express the IU pathway (±IUP) and on whether the culture media were supplemented with unlabeled isoprenol at t = 0 (±ISO). Taxadiene and metabolic intermediate pools were analyzed after 48 h of culture. Shown are concentrations and labeling patterns for metabolic intermediates (*A*) IP, (*B*) IPP/DMAPP, (*C*) GPP, (*D*) FPP, and (*E*) GGPP, respectively. (*F*) Titers of taxadiene produced after 48 h. (*G*) Labeled taxadiene mass spectrum. (*H*) Unlabeled taxadiene mass spectrum. All metabolite and product concentrations are reported as means ± SD of three biological replicates.

were the limiting factor in the production of these isoprenoids, we developed a liquid chromatography-tandem mass spectrometry (LC-MS/MS) method for the detection of intermediates IP, IPP, GPP, FPP, and GGPP and assessed the intracellular metabolites for the pro4IUP taxadiene strain and the pro4IUP p5T7-LYCipi (lycopene) strain using the same type of pulse–chase experiment described earlier. The results indicated that the downstream lycopene flux was still limiting, and optimization of downstream isoprenoid production is necessary to achieve higher titers using the IUP. Even in our highest productivity vector, p5T7-LYCipi, the lycopene cultures were still accumulating significant amounts of IPP (Fig. 4*C*), suggesting that IspA, CrtE (GGPP synthase), CrtB (phytoene synthase), or CrtI (phytoene desaturase) may be limiting enzymes in lycopene synthesis. In taxadiene cultures (Fig. 4*D*), very high levels of GGPP were found to accumulate in the cell, suggesting that taxadiene synthase activity was insufficient to accommodate the high flux generated by the IUP and terpenoid backbone synthesis.

We decided to further investigate the internal metabolites and quantify the contributions of both the IUP and MEP to taxadiene production using pulse–chase labeling experiments (Fig. 5). Taxadiene cultures were grown in M9 media with ^{13}C uniformly labeled glucose as the sole carbon source. Upon reaching OD 0.5, taxadiene production was induced with isopropyl β-D-1-thiogalactopyranoside (IPTG), and, if applicable, isoprenol was added to the media. In these cultures, the IUP plasmid was present or not present (+IUP or –IUP, respectively), and either no isoprenol or 25 mM isoprenol was added (–ISO or +ISO, respectively). After 48 h, the intermediates were extracted and quantified using LC-MS/MS, and taxadiene produced was quantified by GC-MS. As expected, in cultures without isoprenol, no IP (Fig. 5*A*) and very low or undetectable levels of pathway intermediates IPP/DMAPP, GPP, FPP, and GGPP (Fig. 5 *B*–*E*) were found. When isoprenol was supplied to the IUP strain, there was a marked increase in all pathway metabolites, with GGPP accumulating to extremely high levels (600 μmol/g_{dcw} ± 1.89), like previously observed, after 48 h of growth (Fig. 5*E*). The taxadiene produced by the pro4IUP strain supplemented with isoprenol was 96.3% unlabeled (Fig. 5*F*), as confirmed by its mass spectrum (Fig. 5 *G* and *H*). Therefore, taxadiene was almost entirely produced by the IUP from unlabeled isoprenol, and the conversion of GGPP to taxadiene is the rate-limiting step.

Since the lycopene and taxadiene strains, which showed different metabolite accumulation profiles (Fig. 4 *C* and *D*), were identical except for their GGPP synthases and downstream product-synthesis cassettes, we decided to explore the impact of the different GGPP synthases. Whereas lycopene cultures used CrtE derived from *E. agglomerans*, taxadiene cultures employed the homolog GGPPS from *Taxus canadensis*. We created a lycopene vector replacing *crtE* with *ggpps* from *T. canadensis*. The original (CrtE) pro4IUP p5T7-LYCipi strain and the (GGPPS) pro4IUP p5T7-LYCipi-ggpps strain were cultured in batch bioreactors (Fig. 6).

Glucose was depleted within 6 h for the CrtE reactors and 9 h in the GGPPS reactors; however, the GGPPS reactors started with slightly higher glucose at the time of induction (Fig. 6*A*). Lycopene content increased until glucose was depleted (Fig. 6*B*), suggesting that lycopene flux is tied to active growth. The flux observed in the GGPPS reactors was higher than in the CrtE reactors and reached a maximum of 0.430 μmol IPP/min•g_{dcw}, comparable with some of the best reported isoprenoid fluxes (Fig. 6*C*) (29, 30). The maximum lycopene content reached was similar for both cultures and consistent with that observed in serum bottles (Fig. 4*B*). This may suggest that lycopene production from the IUP is limited by the capacity of *E. coli* to store this hydrophobic molecule, which is thought to accumulate in the cell membrane (31).

Discussion

Our main motivation for creating an isoprenoid biosynthesis pathway from a secondary substrate was to circumvent the main challenges that exacerbate attempts at engineering the isoprenoid synthesis pathways. We report the construction of an engineered pathway for the bioconversion of isopentenols, isoprenol, or prenol

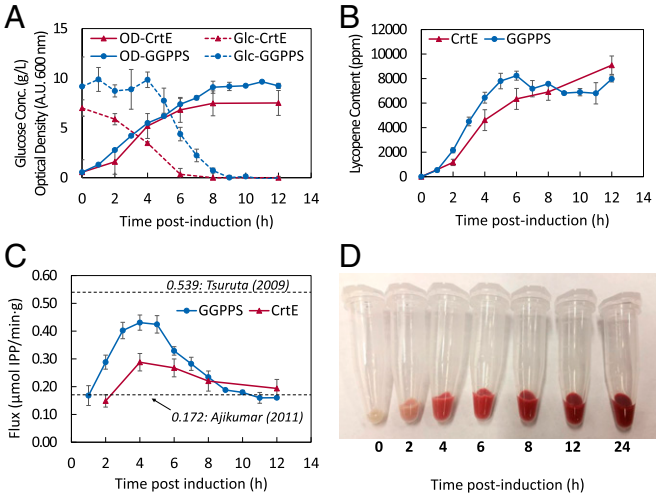

Fig. 6. Batch bioreactor cultivation of lycopene production utilizing the IUP. The IUP was expressed under the control of the pro4 promoter along with a p5T7-LYC vector containing either *crtE* or *ggpps*. (*A*) Glucose concentration and optical density over time. (*B*) Lycopene content over time. (*C*) Cumulative IPP flux calculated from lycopene productivity and comparison with some of the highest reported isoprenoid fluxes (29, 30) in the literature. (*D*) Cell pellets taken from one CrtE bioreactor at different time points. All values represent the mean ± SD based on samples taken from three bioreactor runs. A.U., absorbance units.

to IPP or DMAPP, the main isoprenoid intermediates, and demonstrate the production of several isoprenoids. After minimal optimization of the downstream isoprenoid pathways, an IPP/DMAPP flux, comparable with some of the highest reported, demonstrates the competitiveness of this alternative pathway. The functionality of this pathway hinges on the previously unknown promiscuous activity of choline kinase for the efficient phosphorylation of isoprenol or prenol. Optimization of the combined IUP and downstream product-forming pathway should be much simpler than the current MVA or MEP alternatives. Whereas the latter pathways require multiple unique cofactors and comprise multiple steps, the IUP is much simpler since it only requires a single cofactor (ATP) and is comprised of only two reaction steps. The IUP does not appear to exchange carbon with central metabolism, meaning that it does not have to compete with the rest of the cell for carbon flux. We also note that the downstream cassettes used in this work were unable to accommodate the flux generated by the IUP, shown by large intermediate accumulation, indicating untapped potential. The downstream terpenoid backbone biosynthesis and/or the synthase enzymes should now become the focus of efforts to engineer isoprenoids, rather than achieving an adequate supply of IPP and DMAPP precursors, which has been the major focus of this field for the last 20 y. As such, the isopentenol utilization pathway is an important advancement in the field of isoprenoid biosynthesis.

Materials and Methods

Strains, Plasmids, and Genes. *E. coli* K12 MG1655(DE3) was used as the parent strain for all metabolic pathway expression studies, DH5α (New England Biolabs-NEB) was used for routine cloning purposes, and BL21 (DE3) (NEB) was used for the expression of proteins for purification. Strain genotypes and plasmids used as templates for the construction of the IUP pathway vector and the downstream vectors are listed in *SI Appendix*, Table S1. Genes listed in *SI Appendix*, Table S2 were custom synthesized and codon optimized for *E. coli* MG1655 (Integrated DNA Technologies-IDT) where indicated; otherwise, they were amplified from an existing plasmid or from genomic DNA. Genomic DNA was purified using the Wizard Genomic DNA Purification Kit (Promega Corporation).

Construction of Expression Vectors. All vectors were constructed following the routine cloning protocol described in the *SI Appendix*. Vectors for enzyme expression were constructed by introducing a His-tagged gene (for ScCK, ScMK, EcGK, EcHK, HvIPK, MtIPK, MjIPK, TaIPK, or TaIPK-3m, as defined in Fig. 1*B*, expression) into a pET-28 a (+) vector. Vectors for the expression of the IUP pathway were constructed by incorporating an IUP operon consisting of the genes *Scck*, *ipk*, and *idi* into either a pSEVA228 backbone under the control of the pro4 constitutive promoter (23) for the creation of plasmid pSEVA228-pro4IUPi, or into a pTET backbone (derivative of pET-28a carrying the androtetracycline repressor and promoter region of pBbS2k-rfp) for the creation of plasmid pTET-IUPi. In the case of vector pSEVA228pro4-ck-idi, the IUP operon was lacking gene *ipk*. The lycopene plasmid copy number was varied by amplifying the genes *crtE crtI*, *crtB*, and *ipi*, as well as the endogenous lycopene promoter from plasmid pAC-LYCipi and integrating them in pUC19 and pBR322 backbones to create pUC-LYCipi and p20-LYCipi, respectively. The aforementioned genes were introduced in a pSC101 backbone under a T7 inducible promoter (amplified from p5T7tds-ggpps) to create plasmid p5T7-LYCipi. p5T7-LYCipi-ggpps was created from p5T7-LYCipi by replacing *crtE* with *ggpps*. Plasmids p5T7ispA-ads and p5T7gpps-ls were created by inserting gene pairs *ispA* and *ads* or *ggpps* and *ls*, respectively, into the backbone of p5T7tds-ggpps (pSC101 backbone carrying a T7 inducible promoter/terminator). The full details for the construction of enzyme expression vectors, IUP expression vectors, and downstream isoprenoid pathway expression vectors are provided in *SI Appendix*.

Estimation of IUP Expression Strength. The expression strength for IUP expression vectors pSEVA228-proDIUPi and pTET-IUPi was approximated through characterization using superfolded GFP (sGFP), as reported in ref. 32, as a reporter gene. Derivatives of both IUP expression vectors, containing the sGFP ORF instead of the IUP operon, were created by first PCR amplifying the vector backbone from pSEVA228-proDIUPi using the primer pair GB-pSEVA-back F/R or from pTET-IUPi using the primer pair GB-pTET-back F/R, respectively, and then PCR amplifying the insert fragment containing sGFP from plasmid pTrcsGFP (32) using the primer pairs GB-sGFP-pSEVA F/R or GB-sGFP-pTET F/R, respectively, and finally assembling the respective fragments to give plasmids pSEVA228pro4-gfp and pTET-gfp. To assess the strength of the expression systems, a GFP-based assay, adapted from ref. 23, was used. *E. coli* MG1655 DE3 transformed with either plasmid were grown at 37 °C until reaching midlog phase, at which point GFP fluorescence and OD_{600} was measured [time point 1 (tp1)]. After a further 1.25 h of growth [time point 2 (tp2)], GFP fluorescence and OD_{600} were again assayed, and the GFP synthesis rate, which was used as a proxy for promoter strength, was calculated using the equation: Synthesis rate = $(GFP_{tp2} - GFP_{tp1})/OD_{600,average}$.

Knockout of the Native MEP Pathway. The MEP pathway was knocked out by deleting *ispG* using the CRISPR-cas9 system, in a procedure adapted from refs. 20 and 21. First, pBAD33-proA-MEVI was created by Gibson assembly after PCR amplification of the pBAD33 backbone using primers GB-pBro IAI Vec F/R and amplification of the lower mevalonate pathway from the pMBIS plasmid using primers GB-proX-Mevi F/R. The resulting plasmid, pBAD33-proA-MEV, was created to act as a rescue mechanism for the knockout of *ispG*, which is normally nonviable. The targeting plasmid, pTargetF-ispG, was created by first altering the N20 targeting sequence of the pTargetF plasmid using the primer pair GB-pTargetF-ispGN20_f and GB-ptargetF_N20_r to amplify pTargetF and subsequently circularizing the resulting PCR product with Gibson assembly. The vector was then amplified using the primer pair GB-pTargetF-vec_f/r, and homology regions H1 and H2 were inserted. H1 was designed to encompass the 494 base pairs preceding the *ispG* gene, and H2 was designed to encompass the 501 base pairs after the *ispG* gene. The homology regions were amplified using GB-ispG-H1_f/r and GB-ispG-H2_f/r, respectively. The resulting fragments were then ligated using Gibson assembly. *E. coli* MG1655 (DE3) was transformed with plasmids pBAD33-proA-MEV and pCas9 and plated on a chloramphenicol and kanamycin LB-agar plate overnight. The resulting double transformant was then grown at 30 °C in LB media, which was supplemented with 1 mM D-arabinose at OD_{600} = 0.03. Upon reaching midlog phase, the cells were harvested and washed with glycerol to make them electrocompetent and were then transformed with plasmid pTargetF-ispG and plated overnight at 30 °C on LB-agar plates supplemented with kanamycin, chloramphenicol, spectinomycin, and 1 mM mevalonate. Deletion of *ispG* was confirmed by amplification of the area surrounding *ispG* in the genome using primer pair pCas9-ispG_f/r and sequencing the fragment using primer pCas9-ispG-seq_f. Strain KO1 was obtained by curing the cells of pTargetF-ispG by growing in LB media supplemented with 1 mM IPTG and subsequently curing the cells of pCas9 by growing overnight at 42 °C. Strain KO2 was obtained by making KO1 electrocompetent and transforming with plasmid pSEVA-pro4IUPi. pCas and pTargetF were gifts from Sheng Yang, Chinese Academy of Sciences, Shanghai, China (Addgene plasmids no. 62225 and 62226). pMBIS was a gift from Jay Keasling, University of California, Berkeley, CA (Addgene plasmid # 17817). Mevalonate used in this experiment was produced using the process described in ref. 21 by mixing 1.02 volumes of 2 mM KOH with 1 volume of 2 mM DL-mevalonolactone (Sigma-Aldrich) and incubating at 37 °C for 30 min.

In Vitro Enzyme Assays. Enzyme assays for screening of isopentenol kinase activity were performed as follows. Enzymes were expressed and purified using a protocol detailed in *SI Appendix*. The purified enzymes were added to the enzyme assay master mix for a final concentration of 2 mM ATP, 10 mM $MgCl_2$, 50 mM NH_4HCO_3, pH 7.5, and 600 μM isoprenol or prenol. They were incubated overnight at 37 °C. The reactions were stopped using 5 volumes of ice-cold acetonitrile and centrifuged in an Allegra X-12R centrifuge (Beckman-Coulter) to remove precipitated proteins using a plate adaptor at 3,273 × *g* for 15 min. The supernatant was transferred to a new microplate and frozen at −80 °C. The liquid was removed by a 4.5-L lyophilizer (Labconco), and the samples were resuspended in an equal volume of water and centrifuged again before quantification using LC-MS/MS using a protocol described in *SI Appendix*. Kinetic enzyme assays were conducted using the standard assay conditions described above with the following changes. First, the linear range of the assay was determined over a 90-min period (*SI Appendix*, Fig. S1). Initial velocity appeared linear over this period. Therefore, subsequent kinetic assays were quenched after 30 min. For assays at different temperatures, the standard reaction mixture was used while the temperature was varied using a water bath. For pH optimum, enzymes were buffer-exchanged into 50 mM Tris·HCl at the appropriate pH using 10-kDa nanoseps (Millipore) by exchanging the buffer five times, resulting in a dilution factor of over 10,000. Afterward, reactions were performed in the standard reaction mixture with NH_4HCO_3 buffer adjusted to the appropriate pH. For Michaelis–Menten kinetics, only the concentration of isoprenol or prenol was varied between 1.5 and 50 μM.

Cultivation in Serum Bottles. All media and media additives were prepared according to the manufacturers' recommendations and autoclaved or sterile-filtered (when casamino acids were supplemented) before use. Antibiotics and inducers were filter sterilized and stored as 1,000× solutions at −20 °C until use. Strains were revived from glycerol stocks in LB media (BD) containing the appropriate antibiotic by culturing overnight at 37 °C. Overnight cultures were inoculated at 1% (vol/vol) into 20 mL of M9 media (US Biological Life Sciences) containing 0.32% wt/vol glucose, 0.5% wt/vol casamino acids (Teknova), and ATCC Trace Mineral supplement. When they reached an OD_{600} of 0.5, if necessary, 25 mM (or the specified concentration) isoprenol was added as substrate for the IUP, and/or 10 ng/mL or 20 ng/mL of anhydrotetracycline, as indicated, was added to induce the P_{TET} IUP operon and/or IPTG was added to a final concentration of 100 μM to induce downstream plasmid expression. Strains were cultured in 110-mL serum bottles with rubber stoppers to prevent the evaporation of isoprenol. When strains containing downstream operons for volatile isoprenoid (limonene, amorphadiene, valencene, miltiradiene, and taxadiene) production were used, 100 μL of C18 flash resin (VWR) was added to the cultures at induction time to capture these products. Strains for lycopene and amorphadiene production were grown at 37 °C; otherwise, all cultures were performed at 30 °C. Metabolites, lycopene, and volatile isoprenoids were quantified using protocols described in *SI Appendix*.

Labeling Experiments. Stains used in the pro4 and pTET IUP labeling studies were revived in M9 media with 3.2% wt/vol U-^{13}C glucose. They were then subcultured in the same media and grown until early stationary phase at 37 °C. Samples were taken before the start of the pulse by pipetting 5 mL of culture onto a vacuum filter flask with a 25-mm 0.2-μm nylon filter. The cells were washed with 10 mL of water, and the filter was submerged in ice-cold 80% acetonitrile. At this point, 25 mM isoprenol was added to each culture, and the cultures were sampled at ∼1, 5, 10, 15, 30, 60, and 120 min. Times and optical densities for each point were recorded. IP, IPP, MEP, 3PG, and PEP levels were quantified by LC-MS/MS as described in *SI Appendix*. All trials were performed using three biological replicates. A method described in *SI Appendix* was used to estimate the IUP flux. For taxadiene labeling experiments, the cultures were prepared similarly except they were incubated at 30 °C for 48 h after induction and a C18 flash resin was added. At 48 h, the metabolites were extracted and determined by LC-MS/MS as described in *SI Appendix*. Taxadiene was eluted from the resin and quantified using the GC-MS method described in *SI Appendix*.

Cultivation in Bioreactors. The strains p5T7-LYCipi, p5T7-LYCipi-ggpps, and p5T7tds-ggpps with pro4IUP were cultivated in a 3-L Bioflo 110 bioreactor (New Brunswick) with aeration, agitation, and pH control. One-and-a-half liters of defined media (M9 salts, 5 g/L casamino acids, ATCC trace elements solution, 100 μL of antifoam 204, and 50 μg/mL spectinomycin and kanamycin) were inoculated at 1% vol/vol with an overnight culture (12 h) grown in LB media. Aeration (0.3 to 1 volume of air per volume of liquid per minute) and agitation (250 to 1,250 rpm) were controlled by a cascade to maintain dissolved oxygen at 40% of saturation. pH was controlled by addition of 25% vol/vol NH_4OH. Temperature was controlled at 37 °C for lycopene cultures and 30 °C for taxadiene cultures. When an OD of 0.5 was reached, 1.5 mL of 0.1 M IPTG and 3.75 mL of isoprenol were added. For taxadiene cultures, temperature was reduced to 22 °C after induction. Cell density was monitored by UV/Vis spectroscopy at 600 nm while glucose consumption was determined by HPLC using an Aminex HPX-87H column (300 × 7.8 mm) (Bio-Rad) on an Infinity 1260 series HPLC (Agilent) at a flow rate of 0.7 mL/min with 14 mM H_2SO_4, at room temperature using a refractive index detector set at 50 °C. C18 flash resin was added to taxadiene bioreactors to capture taxadiene and eluted in acetonitrile for purification by semipreparative HPLC as previously described (33).

Data Availability. Data reported in figures are available in *SI Appendix*. Materials can be made available from the corresponding author upon request.

ACKNOWLEDGMENTS. We acknowledge discussions and input from Benjamin Woolston, Nian Liu, Zbigniew Lazar, Lisa Guay, and Bob Van Hove. We thank Benjamin Woolston and Jason King for providing plasmids used in this study. This project was supported by Department of Energy Grants DE-SC 000 8744 and DE-EE 000 7531. V.W. was also supported by the Natural Sciences and Engineering Research Council, Canada. S.M.E. was also supported by a graduate fellowship from the National Science Foundation.

1. Chandran SS, Kealey JT, Reeves CD (2011) Microbial production of isoprenoids. *Process Biochem* 46:1703–1710.
2. Kirby J, Keasling JD (2009) Biosynthesis of plant isoprenoids: Perspectives for microbial engineering. *Annu Rev Plant Biol* 60:335–355.
3. Nagegowda DA (2010) Plant volatile terpenoid metabolism: Biosynthetic genes, transcriptional regulation and subcellular compartmentation. *FEBS Lett* 584: 2965–2973.
4. Liu H, et al. (2013) Combination of Entner-Doudoroff pathway with MEP increases isoprene production in engineered Escherichia coli. *PLoS One* 8:e83290.
5. Chang WC, Song H, Liu HW, Liu P (2013) Current development in isoprenoid precursor biosynthesis and regulation. *Curr Opin Chem Biol* 17:571–579.
6. Zhou K, Zou R, Stephanopoulos G, Too H-P (2012) Metabolite profiling identified methylerythritol cyclodiphosphate efflux as a limiting step in microbial isoprenoid production. *PLoS One* 7:e47513.
7. Banerjee A, et al. (2013) Feedback inhibition of deoxy-D-xylulose-5-phosphate synthase regulates the methylerythritol 4-phosphate pathway. *J Biol Chem* 288: 16926–16936.
8. Nagegowda DA, Bach TJ, Chye M-L (2004) Brassica juncea 3-hydroxy-3-methylglutaryl (HMG)-CoA synthase 1: Expression and characterization of recombinant wild-type and mutant enzymes. *Biochem J* 383:517–527.
9. Brooker JD, Russell DW (1975) Properties of microsomal 3-hydroxy-3-methylglutaryl coenzyme A reductase from Pisum sativum seedlings. *Arch Biochem Biophys* 167: 723–729.
10. Bach TJ, Rogers DH, Rudney H (1986) Detergent-solubilization, purification, and characterization of membrane-bound 3-hydroxy-3-methylglutaryl-coenzyme A reductase from radish seedlings. *Eur J Biochem* 154:103–111.
11. Primak YA, et al. (2011) Characterization of a feedback-resistant mevalonate kinase from the archaeon Methanosarcina mazei. *Appl Environ Microbiol* 77:7772–7778.
12. Kang A, et al. (2016) Isopentenyl diphosphate (IPP)-bypass mevalonate pathways for isopentenol production. *Metab Eng* 34:25–35.
13. King JR, Woolston BM, Stephanopoulos G (2017) Designing a new entry point into isoprenoid metabolism by exploiting fructose-6-phosphate aldolase side reactivity of Escherichia coli. *ACS Synth Biol* 6:1416–1426.
14. Dellas N, Thomas ST, Manning G, Noel JP (2013) Discovery of a metabolic alternative to the classical mevalonate pathway. *eLife* 2:e00672.
15. Gao S, et al. (2008) Substrate promiscuity of pyruvate kinase on various deoxynucleoside diphosphates for synthesis of deoxynucleoside triphosphates. *Enzyme Microb Technol* 43:455–459.
16. Li Y, et al. (2011) Substrate promiscuity of N-acetylhexosamine 1-kinases. *Molecules* 16:6396–6407.
17. Liu Y, Yan Z, Lu X, Xiao D, Jiang H (2016) Improving the catalytic activity of isopentenyl phosphate kinase through protein coevolution analysis. *Sci Rep* 6:24117.
18. Vannice JC, et al. (2014) Identification in Haloferax volcanii of phosphomevalonate decarboxylase and isopentenyl phosphate kinase as catalysts of the terminal enzyme reactions in an archaeal alternate mevalonate pathway. *J Bacteriol* 196: 1055–1063.
19. Chemler JA, Yan Y, Koffas MAG (2006) Biosynthesis of isoprenoids, polyunsaturated fatty acids and flavonoids in Saccharomyces cerevisiae. *Microb Cell Fact* 5:20.
20. Jiang Y, et al. (2015) Multigene editing in the Escherichia coli genome via the CRISPR-Cas9 system. *Appl Environ Microbiol* 81:2506–2514.
21. Martin VJJ, Pitera DJ, Withers ST, Newman JD, Keasling JD (2003) Engineering a mevalonate pathway in Escherichia coli for production of terpenoids. *Nat Biotechnol* 21:796–802.
22. Silva-Rocha R, et al. (2013) The Standard European Vector Architecture (SEVA): A coherent platform for the analysis and deployment of complex prokaryotic phenotypes. *Nucleic Acids Res* 41:D666–D675.
23. Davis JH, Rubin AJ, Sauer RT (2011) Design, construction and characterization of a set of insulated bacterial promoters. *Nucleic Acids Res* 39:1131–1141.
24. Lee TS, et al. (2011) BglBrick vectors and datasheets: A synthetic biology platform for gene expression. *J Biol Eng* 5:12.
25. Takehara M, et al. (2014) Characterization and thermal isomerization of (all-E)-lycopene. *J Agric Food Chem* 62:264–269.
26. Davis WB (1949) Preparation of lycopene from tomato paste for use as a spectrophotometric standard. *Anal Chem* 21:1226–1228.
27. Srivastava S, Srivastava AK (2015) Lycopene; chemistry, biosynthesis, metabolism and degradation under various abiotic parameters. *J Food Sci Technol* 52:41–53.
28. Cunningham FX, Jr, Lee H, Gantt E (2007) Carotenoid biosynthesis in the primitive red alga Cyanidioschyzon merolae. *Eukaryot Cell* 6:533–545.
29. Ajikumar PK, et al. (2010) Isoprenoid pathway optimization for taxol precursor overproduction in Escherichia coli. *Science* 330:70–74.
30. Tsuruta H, et al. (2009) High-level production of amorpha-4,11-diene, a precursor of the antimalarial agent artemisinin, in Escherichia coli. *PLoS One* 4:e4489.
31. Wang GS, Grammel H, Abou-Aisha K, Sägesser R, Ghosh R (2012) High-level production of the industrial product lycopene by the photosynthetic bacterium Rhodospirillum rubrum. *Appl Environ Microbiol* 78:7205–7215.
32. Santos CNS, Koffas M, Stephanopoulos G (2011) Optimization of a heterologous pathway for the production of flavonoids from glucose. *Metab Eng* 13: 392–400.
33. Edgar S, et al. (2016) Mechanistic insights into taxadiene epoxidation by taxadiene-5α-hydroxylase. *ACS Chem Biol* 11:460–469.